Structural Eng. / Earthquake Eng. Vol. 4. No. 1, 31 s-40 s. April 1987
Japan Society of Civil Engineers (Proc. of JSCE No. 380/I-7)

ANALYSIS OF ELASTIC DISTORTIONAL INSTABILITY OF THIN-WALLED MEMBERS WITH OPEN POLYGONAL CROSS SECTION

By Hiroshi HIKOSAKA, Katsuhiko TAKAMI** and Yoshikazu MARUYAMA****

A new method is presented for analyzing the interaction between local and overall instability of thin-walled open polygonal section members. Based on beam theory approximations, non-linear expressions for displacements are first derived taking the distortion of cross section into account, and then the governing equations for instability of members are developed. Buckling loads for I-section beam and hat-section column are analyzed as examples, and the accuracy of the method is discussed by comparing some solutions with those obtained using the more complex method based on plate theory. The method makes it possible to predict the local through distortional to lateral instability of members using a small number of degrees of freedom.

Keywords : finite displacement theory, instability, distortion.

1. INTRODUCTION

Thin-walled members are used extensively in structures since they provide an economical use of material for the provision of stiffness and strength. The structural behavior of thin-walled members of open cross section is, however, very complex because they are susceptibie to geometrically non-linear behavior and to instability in a variety of modes.

The usual methods for analyzing the deformation and instability of structural members assume that the cross sections remain undistorted. However, when a member is thin-walled, distortion may occur during deformation and consequently its rigidity may be reduced. The distortional deformation and instability occur in a mode in which lateral deflection and twist are combined with general distortions of the cross sectional shape. Plate buckling of components in a thin-walled member, normally called local buckling, results in distortion without overall member buckling. Instability of a combination of local and overall member buckling is called the distortional instability. The distortional mode occurs at a longer wave length than the local buckling mode, and distortional effects may also lower the critical load for the overall member buckling.

The FEM (Finite Element Method) based on plate theory approximation is able to take account of any deformation including distortion of cross section, although the analysis becomes relatively time-consuming and expensive. The FSM (Finite Strip Method) is more efficient than, but not as general as, the FEM. However, the FSM again leads to a comparatively time-consuming analysis for folded plate systems, since it usually uses four degrees of freedom per nodal line.

* Member of JSCE, Dr. Eng., Professor of Civil Engineering, Kyushu University (Hakozaki 6-10-1, Higashi-ku, Fukuoka).
** Member of JSCE, M. Eng., Research Associate, Department of Civil Engineering, Kyushu University.
*** Student Member of JSCE, M. Eng., Graduate Student, Department of Civil Engineering, Kyushu University.

In this paper, a method is presented for analyzing the interaction between the local, distortional and overall instability of thin-walled members of open polygonal cross section. Based on not plate theory but beam theory approximations, non-linear expressions for the displacements and strains under distortion of cross section are derived. After neglect of third- and higher-order terms in the displacements, the governing equations for studying various elastic instabilities of members are developed. The method can greatly reduce the number of degrees of freedom in the analysis, achieving satisfactory accuracy of the solution.

2. COORDINATE SYSTEMS AND DEFINITION OF DISTORTION

A thin-walled member with polygonal cross section is shown in Fig. 1. The z-axis is the longitudinal centroidal axis, while x and y axes are the principal axes. The shear center of the section is denoted by S (x_s, y_s). To define the geometry of the cross section, we estabish an another orthogonal curvilinear coordinate system (n, s). The tangential coordinate s is measured counterclockwise along the center line of the wall, and n is in the direction of outward normal to s. The wall thickness t is a function of s.

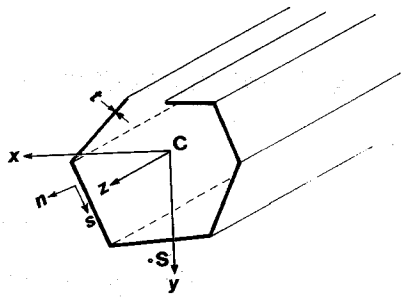

Fig. 1 Coordinate system of thin-walled member.

Let us consider a thin-walled section consisting of N plate elements whose junctions are numbered 1, 2, ···, N−1 as shown in Fig. 2. Distortion of the cross section is defined by a combination of translation and twist of each plate accompanied with its transverse bending, while the effect of its transverse stretching on the distortion is neglected. In the case when it is necessary to consider more accurately the local buckling behavior of any compressed plate element, we divide it into two or more elements. It has been shown to be satisfactory in previous studies[1)~4)] that the local buckling behavior of end plates having one or two free edges, such as plate 1 and N in Fig. 2, can be accurately predicted by assuming them to be rigid.

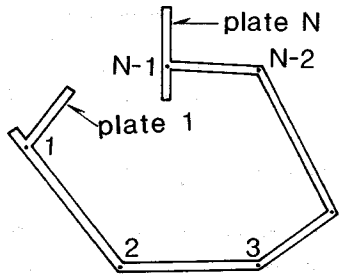

Fig. 2 Plate elements and nodes.

For the analysis in this paper, the components of distortion are defined only by the relative rotation or the change of angle between adjacent plate elements, $\theta_1, \theta_2, \cdots, \theta_{N-1}$. Fig. 3 shows the definition of the relative rotation θ_i, which is assumed positive when the plate i rotates counterclockwise from the plate i+1. As a result of this treatment, an open section member consisting of N plates has N−1 degrees of freedom for distortion.

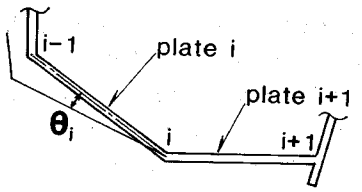

Fig. 3 Definition of distortion.

3. NON-LINEAR DISPLACEMENTS AND STRAINS IN DISTORTION

The following assumptions are made in the present theory : (i) shear strain due to non-uniform bending can be neglected, and (ii) displacemtns in the x and y directions are much larger than the displacement in the z direction.

Let u, v and w denote the displacements of any point P(x, y, z) in the x, y and z directions, respectively. In the finite displacement theory taking account of the assumption (ii), the strain-displacement relations are given by[5)]

$$\left.\begin{aligned}&\varepsilon_z=\frac{\partial w}{\partial z}+\frac{1}{2}\left\{\left(\frac{\partial u}{\partial z}\right)^2+\left(\frac{\partial v}{\partial z}\right)^2\right\},\quad \gamma_{yz}=\frac{\partial w}{\partial y}+\frac{\partial v}{\partial z}+\frac{\partial u}{\partial y}\frac{\partial u}{\partial z}+\frac{\partial v}{\partial y}\frac{\partial v}{\partial z}\\&\gamma_{zx}=\frac{\partial u}{\partial z}+\frac{\partial w}{\partial x}+\frac{\partial u}{\partial z}\frac{\partial u}{\partial x}+\frac{\partial v}{\partial z}\frac{\partial v}{\partial x}\end{aligned}\right\}\quad\cdots\cdots\cdots\cdots\cdots\cdots\cdots\cdots\quad(1\cdot a\sim c)$$

where ε_z is axial strain and γ_{yz}, γ_{zx} are shear strains.

If no cross section of a member is distorted at all during deformation, the displacements of any point P in the $x-y$ plane are completely specified by three components u_s, v_s and ϕ, in which u_s and v_s denote displacements of the shear center S in the x and y directions and ϕ denotes the rotation of the section about the shear center. When the cross section is distorted, on the other hand, the total displacements will be discribed by relative rotations of the wall elements, θ_i (i=1, 2, ···, N−1), in addition to rigid body movements u_s, v_s and ϕ.

Let s_i be the curvilinear coordinate of the point i(x_i, y_i) located at the junction of the plate i and i+1, as shown in Fig. 4 and let μ_i be the unit step function defined by

$$\mu_i=\begin{cases}1 & (s\leqq s_i)\\ 0 & (s>s_i)\end{cases}$$

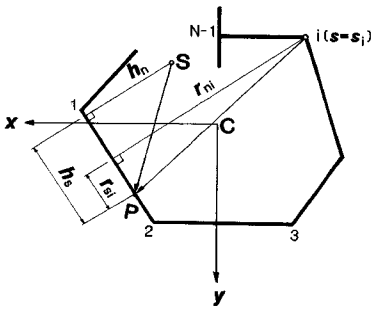

Fig. 4 Geometry of cross section.

Then, from simple geometry, the finite displacements u and v in Eqs. (1) can be derived as follows:

$$\left.\begin{aligned}u&=u_s-(y-y_s)\sin\phi-(x-x_s)(1-\cos\phi)+u_0\cos\phi-v_0\sin\phi\\v&=v_s+(x-x_s)\sin\phi-(y-y_s)(1-\cos\phi)+u_0\sin\phi+v_0\cos\phi\end{aligned}\right\}\quad\cdots\cdots\cdots\cdots\cdots\cdots\cdots\cdots\quad(2)$$

in which

$$\left.\begin{aligned}u_0&=-\sum_{i=1}^{N-1}\{(y-y_i)\sin\theta_i+(x-x_i)(1-\cos\theta_i)\}\mu_i\\v_0&=\sum_{i=1}^{N-1}\{(x-x_i)\sin\theta_i-(y-y_i)(1-\cos\theta_i)\}\mu_i\end{aligned}\right\}\quad\cdots\cdots\cdots\quad(3)$$

If u_0 and v_0 are neglected in Eqs. (2), the formulas for u and v represent the finite displacements for undistorted members[5]. Substituting Eqs. (3) into Eqs. (2) and neglecting third- and higher-order terms which appear in the resulting equations, we obtain the following second-order expressions for displacements:

$$\left.\begin{aligned}u&=u_s-(y-y_s)\phi-\frac{1}{2}(x-x_s)\phi^2-\sum_{i=1}^{N-1}\left\{(x-x_i)\left(\phi+\frac{\theta_i}{2}\right)+(y-y_i)\right\}\theta_i\mu_i\\v&=v_s+(x-x_s)\phi-\frac{1}{2}(y-y_s)\phi^2+\sum_{i=1}^{N-1}\left\{(x-x_i)-(y-y_i)\left(\phi+\frac{\theta_i}{2}\right)\right\}\theta_i\mu_i\end{aligned}\right\}\quad\cdots\cdots\cdots\cdots\cdots\cdots\cdots\quad(4)$$

Referring to Fig. 4, s and n components of the vector drawn from S to P are denoted h_s and h_n, respectively, and those drawn from i to P are r_{si} and r_{ni}, respectively. Now let w_c denote the displacement of the centroid C in the z direction, and let s_c and μ_{ic} be the values of s and μ_i at the centroid. Introducing Eqs. (4) into the equations $\gamma_{yz}=\gamma_{zx}=0$ under the assumption (i), then we can derive the longitudinal displacement w in the following form:

$$w=w_c-(u_s'+v_s'\phi)x-(v_s'-u_s'\phi)y+\omega\phi'+\sum_{i=1}^{N-1}\left\{\phi_i\theta_i'+\left(\alpha_i u_s'-\beta_i v_s'+\lambda_i\phi'+\sum_{j=1}^{N-1}\kappa_{ji}\theta_j'\right)\theta_i\right\}\quad\cdots\cdots\cdots\quad(5)$$

where

$$\left.\begin{aligned}&\omega=\int_s^{s_c}h_n ds+nh_s,\quad \phi_i=\int_s^{s_c}r_{ni}\mu_i ds+nr_{si}\mu_i,\quad \lambda_i=\int_s^{s_c}(h_s-r_{si})\mu_i ds-n(h_n-r_{ni})\mu_i\\&\alpha_i=(y-y_i)\mu_i+y_i\mu_{ic},\quad \beta_i=(x-x_i)\mu_i+x_i\mu_{ic},\quad \kappa_{ji}=\int_s^{s_c}r_{si}\mu_i\mu_j ds-nr_{ni}\mu_i\mu_j\end{aligned}\right\}\quad\cdots\cdots\cdots\quad(6)$$

κ_{ji} in Eqs. (6) is defined only for i≠j, and $\kappa_{ji}=0$ for i=j. In Eq. (5) and throughout the present paper,

the prime denotes differentiation with respect to z, that is $(\ )'=d(\ )/dz$. The first terms in the right hand side of formulas for ω and ϕ_i in Eqs. (6) are primary warping functions for thin-walled open section members, and the second terms of them represent secondary warping effects which cannont necessarily be neglected in the local buckling of shorter wave length[3].

Non-linear axial strain ε_z is derived by substitution of Eqs. (4) and (5) into Eq. (1·a) and shear strain γ_{zs} due to St. Venant torsion is given by

$$\gamma_{zs}=2n\left(\phi'+\sum_{i=1}^{N-1}\mu_i\theta_i'\right) \quad (7)$$

The axial stress σ_z and shear stress τ_{zs} corresponding to strains ε_z and γ_{zs} are:

$$\sigma_z=E\varepsilon_z, \quad \tau_{zs}=G\gamma_{zs} \quad (8\cdot a, b)$$

where E is Young's modulus and G is shear modulus.

4. TRANSVERSE BENDING MOMENT AND STRESS OF WALL ELEMENTS

Let a segment of unit width be cut out from a thin-walled member by two adjacent cross sections, as shown in Fig. 5. We treat it as a polygonal frame consisting of N members of flexural rigidity EI_s ($I_s=t^3/12$, where t is wall thickness). Then, the transverse bending moment M_s is related to the rotations θ_i (i $=1, 2, \cdots, N-1$) by the linear expression

$$M_s=\sum_{i=1}^{N-1}M_i\theta_i \quad (9)$$

where M_i is the bending moment of the frame obtained by setting all rotations equal to zero except θ_i, and $\theta_i=1$. Examples of transverse bending for I-section member are illustrated later in Fig. 6.

M_s produces the transverse stress σ_s and strain ε_s given by

$$\sigma_s=\frac{M_s}{I_s}n, \quad \varepsilon_s=\frac{\sigma_s}{E} \quad (10\cdot a, b)$$

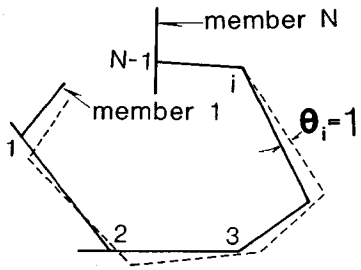

Fig. 5 Transverse bending.

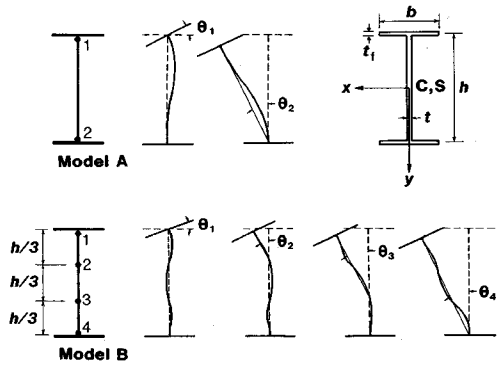

Fig. 6 Analytical models for I-section member.

5. EQUILIBRIUM EQUATIONS AND BOUNDARY CONDITIONS

We denote the x, y, z components of external forces per unit length in a thin-walled member by q_x, q_y, q_z, respectively, and the intensity of external torque per unit length by m_z. On the boundary cross sections at $z=0$ and $z=L$, the member is subjected to a general system of applied loads or end reactions: two shearing forces $\overline{V}_x$ and $\overline{V}_y$ acting parallel to the section, a normal force $\overline{N}_z$, two moments $\overline{M}_x$ and $\overline{M}_y$ acting about the x and y axes, and a torque $\overline{M}_z$ acting about the z axis. Then, the equilibrium state of the member is expressed by the principle of virtual work as follows:

$$\int_0^L\int_A(\sigma_z\delta\varepsilon_z+\tau_{zs}\delta\gamma_{zs}+\sigma_s\delta\varepsilon_s)dAdz=\int_0^L(q_x\delta u_s+q_y\delta v_s+q_z\delta w_c+m_z\delta\phi)dz$$

$$+[n_z\{\overline{V}_x\delta u_s+\overline{V}_y\delta v_s+\overline{N}_z\delta w_c+\overline{M}_y\delta(u_s'+v_s'\phi)-\overline{M}_x\delta(v_s'-u_s'\phi)+\overline{M}_z\delta\phi\}]_0^L \cdots\cdots (11)$$

where the symbol δ is a variational operator, A is cross sectional area of the member, $n_z=-1$ at $z=0$ and $n_z=1$ at $z=L$.

Substituting Eqs. (4), (5), (8) and (10) into Eq. (11) gives the final expression of Eq. (A·1) in Appendix, and then the governing differential equations and the boundary conditions can be derived by virtue of the variational principle. The integration over the area A in the left hand side of Eq. (11) yields a system of stress resultants defined by

$$N_z=\int_A\sigma_z dA,\quad M_x=\int_A\sigma_z y dA,\quad M_y=\int_A\sigma_z x dA,\quad M_\omega=\int_A\sigma_z\omega dA,\quad T_s=\int_A\tau_{zs}(2n)dA \cdots\cdots (12\cdot a)$$

$$M_{\omega i}=\int_A\sigma_z\phi_i dA,\quad T_{si}=\int_A\tau_{zs}(2n)\mu_i dA,\quad F_{si}=\int_A\sigma_s\frac{M_i}{EI_s}ndA \cdots\cdots (12\cdot b)$$

Although some more general stress resultants are defined in the theory[6], they are not used in the problems of instability discussed herein, and therefore they have been omitted for simplicity in this paper. The governing equations applied for the problems of distortional buckling are shown in the following section.

6. DISTORTIONAL INSTABILITY ANALYSIS

(1) Force-displacement relations in the small displacement theory[9),10)]

In the small displacement theory where the non-linear terms are neglected, the axial stress σ_z in Eq. (8·a) can be written as

$$\sigma_z=E\left(w_c'-xu_s''-yv_s''+\omega\phi''+\sum_{i=1}^{N-1}\phi_i\theta_i''\right) \cdots\cdots (13)$$

Introducing Eqs. (8·b), (10·a) and (13) into Eqs. (12), the linear stress resultants in the small displacement theory can be expressed as the functions of displacements in the following form:

$$\left.\begin{aligned} &N_z=EAw_c'+\sum_{j=1}^{N-1}EH_{j0}\theta_j'',\quad M_x=-EI_xv_s''+\sum_{j=1}^{N-1}EH_{jx}\theta_j''\\ &M_y=-EI_yu_s''+\sum_{j=1}^{N-1}EH_{jy}\theta_j'',\quad M_\omega=EI_\omega\phi''+\sum_{j=1}^{N-1}EH_{j\omega}\theta_j''\\ &T_s=GJ\phi'+\sum_{j=1}^{N-1}GJ_j\theta_j' \end{aligned}\right\} \cdots\cdots (14\cdot a)$$

$$\left.\begin{aligned} &M_{\omega i}=E\left\{H_{i0}w_c'-H_{iy}u_s''-H_{ix}v_s''+H_{i\omega}\phi''+\sum_{j=1}^{N-1}H_{ij}\theta_j''\right\}\\ &T_{si}=GJ_i\phi'+\sum_{j=1}^{N-1}GJ_{ij}\theta_j',\quad F_{si}=\sum_{j=1}^{N-1}f_{ij}\theta_j \end{aligned}\right\} \cdots\cdots (14\cdot b)$$

where

$$\left.\begin{aligned} &A=\int_A dA,\quad I_x=\int_A y^2dA,\quad I_y=\int_A x^2dA,\quad I_\omega=\int_A\omega^2dA,\quad J=\int_s(t^3/3)ds\\ &H_{i0}=\int_A\phi_i dA,\quad H_{ix}=\int_A\phi_i y dA,\quad H_{iy}=\int_A\phi_i x dA,\quad H_{i\omega}=\int_A\phi_i\omega dA,\quad H_{ij}=\int_A\phi_i\phi_j dA\\ &f_{ij}=\int_s\frac{M_iM_j}{EI_s}ds,\quad J_i=\int_s(t^3/3)\mu_i ds,\quad J_{ij}=\int_s(t^3/3)\mu_i\mu_j ds \end{aligned}\right\} \cdots\cdots (15)$$

(2) Governing equations for distortional instability

Let us now examine the application of the theory presented herein to some simple problems. By using small but finite increments in displacements, stresses and strains such that the member moves to an adjacent equilibrium state, Eq. (11) can be rewritten in the form of incremental expression. And then, the incremental equation thus obtained and the linear force-displacement relations in Eqs. (14) facilitate a study of the elastic distortional instability of thin-walled members.

Consider a simply supported member subjected to compressive axial force P through its centroid and to

uniform bending moment M_0 applied in the yz plane. P and M_0 produce stresses in the member prior to buckling which are given by

$$\sigma_z^{(0)}=-\frac{P}{A}+\frac{M_0}{I_x}y \quad \cdots\cdots (16)$$

Then, the linearlized equilibrium equations for the elastic instability can be derived as follows:

$$\left.\begin{aligned}
&-M_y''+M_0\phi''+P(u_s''+y_s\phi'')+\sum_{i=1}^{N-1}M_{xi}^{(0)}\theta_i''=0\\
&-M_x''+P(v_s''-x_s\phi'')-\sum_{i=1}^{N-1}M_{yi}^{(0)}\theta_i''=0\\
&M_\omega''-T_s'+P(y_su_s''-x_sv_s'')+M_0u_s''-K^{(0)}\phi''-\sum_{i=1}^{N-1}L_i^{(0)}\theta_i''=0\\
&M_{\omega i}''-T_{si}'+F_{si}+M_{xi}^{(0)}u_s''-M_{yi}^{(0)}v_s''-L_i^{(0)}\phi''-\sum_{j=1}^{N-1}K_{ij}^{(0)}\theta_j''=0\\
&\qquad (i=1,2,\cdots,N-1)
\end{aligned}\right\} \quad \cdots\cdots (17)$$

where M_x, M_y, M_ω, T_s, $M_{\omega i}$, T_{si}, F_{si} are given by Eqs. (14), and

$$\left.\begin{aligned}
&K^{(0)}=\int_A\sigma_z^{(0)}r_p^2dA,\quad M_{xi}^{(0)}=\int_A\sigma_z^{(0)}(y-y_i)\mu_idA,\quad M_{yi}^{(0)}=\int_A\sigma_z^{(0)}(x-x_i)\mu_idA\\
&L_i^{(0)}=\int_A\sigma_z^{(0)}(h_nr_{ni}+h_sr_{si})\mu_idA,\quad K_{ij}^{(0)}=\int_A\sigma_z^{(0)}r_{ij}\mu_i\mu_jdA\\
&r_p^2=(x-x_s)^2+(y-y_s)^2,\quad r_{ij}=(x-x_i)(x-x_j)+(y-y_i)(y-y_j)
\end{aligned}\right\} \quad \cdots\cdots (18)$$

The boundary conditions are, at $z=0$ and L,

$$u_s=v_s=\phi=\theta_i=u_s''=v_s''=\phi''=\theta_i''=0 \quad \cdots\cdots (19)$$

(3) Distortional instability of I-section beam subjected to uniform bending

Eqs. (17) have been applied to analyze the elastic buckling of symmetrical I-section members bent about their major axis in uniform bending. Two analytical models shown in Fig. 6 have been used to investigate the effect of different degrees of freedom: the Model A has only two nodal lines at the junctions between web and flanges, the Model B has two more nodal lines in the web, and the flanges were assumed to be rigid in both Models A and B.

For the symmetrical I-section beam under consideration, the shear center coincides with the centroid, i.e., $x_s=y_s=0$, and terms containing P, $K^{(0)}$, $M_{yi}^{(0)}$ and v_s vanish in Eqs. (17). Then, substituting Eqs. (14) into Eqs. (17) gives

$$\left.\begin{aligned}
&EI_yu_s''''+M_0\phi''+\sum_{j=1}^{N-1}(-EH_{iy}\theta_j''''+M_{xi}^{(0)}\theta_j'')=0\\
&M_0u_s''+EI_\omega\phi''''-GJ\phi''+\sum_{j=1}^{N-1}\{EH_{i\omega}\theta_j''''-(GJ_j+L_j^{(0)})\theta_j''\}=0\\
&-EH_{iy}u_s''''+M_{xi}^{(0)}u_s''+EH_{i\omega}\phi''''-(GJ_i+L_i^{(0)})\phi''+\sum_{j=1}^{N-1}\{EH_{ij}\theta_j''''-(GJ_{ij}+K_{ij}^{(0)})\theta_j''+f_{ij}\theta_j\}=0\\
&\qquad (i=1,2,\cdots,N-1)
\end{aligned}\right\} \quad \cdots\cdots (20)$$

where N=3 for the Model A and N=5 for the Model B.

In general, a beam may buckle in a number of half waves. Displacement functions which satisfy the prescribed boundary conditions in Eqs. (19) are:

$$u_s=C_1\sin\frac{m\pi}{L}z,\quad \phi=C_2\sin\frac{m\pi}{L}z,\quad \theta_i=C_{2+i}\sin\frac{m\pi}{L}z \quad \cdots\cdots (21)$$
$$(m=1,2,\cdots,\infty)$$

where C_1, C_2, $\cdots$, C_{N+1} are constants yet to be determined, and m represents the number of half wave length of buckle over the length of the beam. Substituting Eqs. (21) into Eqs. (20) and using the technique for eigenvalue analysis, the solution for the critical moment M_0 can be obtained.

For the purpose of demonstrating the accuracy of the solutions obtained by the present theory, the cross

sections analyzed by the FEM in Ref. 7) were used as examples. In the FSM analysis, both the compression flange and web were divided into four strips, and the tension flange was divided into two strips. This subdivision in the FSM would be sufficient to produce error less than 1 %.

The non-dimensional critical moments for beams with two different cross-sectional shapes, whose dimensions are shown in Figs. 7(a) and 7(b), have been calculated using the first mode, $m=1$, in Eqs. (21), and are plotted in Fig. 7 for a variety of beam length L. The section for Fig. 7(b) has the same dimension as the section for Fig. 7(a) except that the web thickness has been reduced to half. The non-dimensional critical moment is defined by $\overline{M}_{cr}=M_0/EW$, where E is Young's modulus and W is the section modulus for the center line of the flange. The range I, II and III for the ratio L/h in Fig. 7 correspond to the local, distortional and lateral instability, respectively, which can be distinguised by both the buckling mode of cross section and the change of curvature in $\overline{M}_{cr}-L/h$ curve.

In Fig. 7(a), region I corresponds to a local buckle of compression flange interacting with the compression zone in the web. The same region in Fig. 7(b) corresponds, however, to a local buckle of the web elastically restrained by the stockier flanges. In both figures, region III corresponds to a lateral-torsional buckle with no significant distortion of the cross section. In region II, distortion is taking place to produce a coupling between the local and lateral-torsional modes.

The estimate for critical moment, calculated by the present theory using the Model B, is very close to the FSM solution in both Figs. 7(a) and 7(b). The Model A can predict the critical moment involving the mode of local flange buckling in Fig. 7(a), but the value of critical moment determined using the same model in Fig. 7(b) is significantly higher because the modes of local web buckling cannot be included in the Model A.

Thus, the Model B can give a continuous transformation of critical moment from local through distortional to lateral buckling, using extremely smaller number of degrees of freedom than the FSM. In Fig. 8, the critical moments versus beam length are plotted for $m=1, 2, 3, \cdots$. The envelope of the lowest points on these curves defines the minimum critical moment versus beam length.

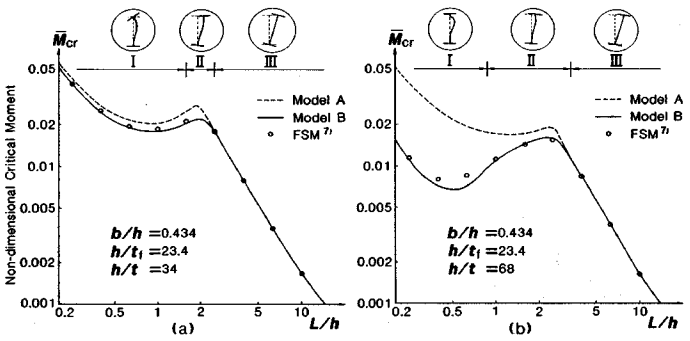

Fig. 7 Critical moment versus beam length (m=1).

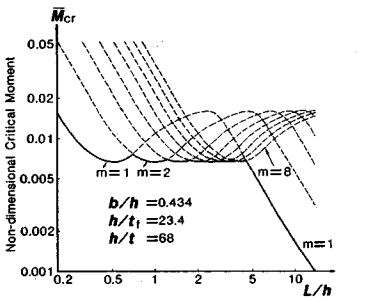

Fig. 8 Critical moment versus beam length (Model B).

(4) Distortional instability of hat-section column under axial compression

Another application of Eqs. (17) is now illustrated by considering a combination of flexural buckling about the x-axis and symmetrical distortion, for hat-section column under axial compression, as shown in Fig. 9(a). Combined torsional and flexural buckling accompanied by antisymmetrical distortion may also be possible to occur in this case, but it is not treated here.

Two foundamentally different local buckling modes characterize the behavior of hat-section stub column, as shown schematically in Fig. 10[8]. One is the local plate buckling mode, where instability is initiated by local buckling of the plate elements, as though they are supported along their junctions. The other is the flange buckling mode, where instability is initiated by buckling of the upper flange in the x direction. For

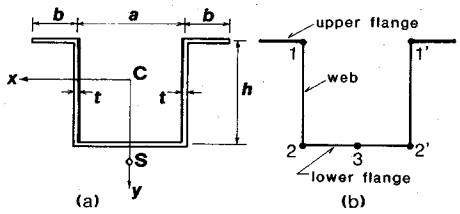

Fig. 9 Analytical model for hat-section column.

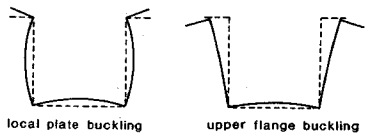

Fig. 10 Local buckling modes of hat-section.

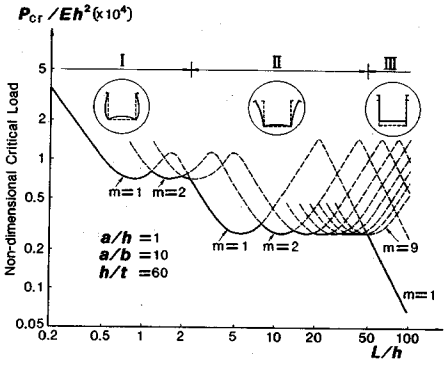

Fig. 11 Critical load versus column length.

the latter mode, instability of the upper flange will necessarily induce simultaneous local buckling of the web. When the column length is not sufficiently short to prevent overall buckling, however, combined local and flexural buckling may occur.

The cross section was divided into five elements as shown in Fig. 9(b), so that two fundamental local buckling modes can be taken into account in the model. Since we deal with only the symmetrical distortion, the section has three degrees of freedom for distortion. The shear center is located on the y-axis, i. e., $x_s=0$, and terms containing M_0, $M_{xi}^{(0)}$, $L_i^{(0)}$, u_s and ϕ vanish in Eqs. (17). Then, substituting Eqs. (14) into Eqs. (17) gives

$$\left.\begin{aligned} &EI_x v_s''''+P v_s''-\sum_{j=1}^{3}(EH_{jx}\theta_j''''+M_{yj}^{(0)}\theta_j'')=0 \\ &-EH_{ix}v_s''''-M_{yi}^{(0)}v_s''+\sum_{j=1}^{3}\left\{E\left(H_{ij}-\frac{H_{i0}H_{j0}}{A}\right)\theta_j''''-(GJ_{ij}+K_{ij}^{(0)})\theta_j''+f_{ij}\theta_j\right\}=0 \\ &\qquad\qquad (i=1,2,3) \end{aligned}\right\} \quad \cdots\cdots (22)$$

Displacement functions which satisfy the pinned-end conditions are :

$$v_s=C_1\sin\frac{m\pi}{L}z, \quad \theta_i=C_{1+i}\sin\frac{m\pi}{L}z \quad \cdots\cdots (23)$$
$$(m=1,2,\cdots,\infty)$$

Substituting Eqs. (23) into Eqs. (22) and proceeding the eigenvalue analysis, the critical load, P_{cr}, for combined distortional and flexural buckling can be obtained.

The non-dimensional critical loads, P_{cr}/Eh^2, are plotted in Fig. 11 for a variety of length L of the column, whose geometry is shown in the figure. Region I and II correspond to the local plate buckling and the flange buckling in Fig. 10, respectively, and Region III corresponds to the Euler buckling about the x-axis with no significant distortion of the cross section. Each curve in Fig. 11 represent a different number of buckling waves, and the envelope of the lowest points on these curves defines a graph of minimum buckling load versus column length.

7. CONCLUDING REMARKS

A method of analyzing the elastic distortional instability of thin-walled members with open cross section has been presented in this paper.

At first, non-linear behavior of members based on the second-order finite displacement thoery was formulated, and then the governing equations for the instability of members were developed. Since the method uses only one degree of freedom at each node to specify the distortion of cross section, it can greatly reduce the complexity arising in the finite element or finite strip metod.

Following the development of the theory, the method has been used to demonstrate the interaction between the local, distortional, and overall buckling modes of the I-section beam in uniform bending and of the hat-section column under axial compression. The numerical solutions were compared with those by the finite strip method, and the close agreement between the two solutions justifies the formulation presented herein.

The method has made it possible to predict accurately the elastic buckling loads from local through distortional to lateral instability by using a small number of degrees of freedom. Elastic critical loads are used, however, mainly as reference loads, relative to which actual failure loads or general patterns of behavior can be assessed. Since all real structures have small geometric imperfections, it is necessary to further extend the method considering both geometric and material non-linearities in a realistic analysis. The method of formulation presented in this paper will still be useful in such a case, because it will require relatively few degrees of freedom to achieve satisfactory convergence of the solution.

APPENDIX : Final Result of Eq. (11)

Integrating Eq. (11) by parts gives the following virtual work equation :

$$
\begin{aligned}
&-\int_0^L \Big\{(N'_z+q_z)\delta w_c+(V'_x+q_x)\delta u_s+(V'_y+q_y)\delta v_s+(M'_z-M_x u''_s+M_y v''_s+m_z)\delta\phi \\
&\quad+\sum_{i=1}^{N-1}(M'_{zi}-F_{si}-M_{xi}u''_s+M_{yi}v''_s)\delta\theta_i\Big\}dz+\Big[(N_z-n_z\overline{N}_z)\delta w_c+(V_x-n_z\overline{V}_x)\delta u_s \\
&\quad-[M_y-M_x\phi+n_z(\overline{M}_y+\overline{M}_x\phi)-\sum_{i=1}^{N-1}\{M_{xi}+y_i\mu_{ic}(N_z-n_z\overline{N}_z)\}\theta_i]\delta u'_s+(V_y-n_z\overline{V}_y)\delta v_s \\
&\quad-[M_x+M_y\phi-n_z(\overline{M}_x-\overline{M}_y\phi)+\sum_{i=1}^{N-1}\{M_{yi}+x_i\mu_{ic}(N_z-n_z\overline{N}_z)\}\theta_i]\delta v'_s+\{M_z-n_z(\overline{M}_z+\overline{M}_x u'_s+\overline{M}_y v'_s)\}\delta\phi \\
&\quad+M_\omega\delta\phi'+\sum_{i=1}^{N-1}\{M_{zi}+\mu_{ic}(N_z-n_z\overline{N}_z)(y_i u'_s-x_i v'_s)\}\delta\theta_i+\sum_{i=1}^{N-1}M_{\omega i}\delta\theta'_i\Big]_0^L=0 \qquad \cdots\cdots (A\cdot1)
\end{aligned}
$$

in which a system of stress resultants N_z, M_x, M_y, M_ω, $M_{\omega i}$, and F_{si} have been defined in Eqs. (12), and

$$
\left.
\begin{aligned}
&M_{xi}=\int_A \sigma_z(y-y_i)\mu_i dA, \quad M_{yi}=\int_A \sigma_z(x-x_i)\mu_i dA \\
&V_x=(M_y-M_x\phi)'+N_z(u'_s+y_s\phi')-\sum_{i=1}^{N-1}(M_{xi}\theta_i)' \\
&V_y=(M_x+M_y\phi)'+N_z(v'_s-x_s\phi')+\sum_{i=1}^{N-1}(M_{yi}\theta_i)' \\
&M_z=T_s-M'_\omega+K\phi'+N_z(y_s u'_s-x_s v'_s)+\sum_{i=1}^{N-1}L_i\theta'_i \\
&M_{zi}=T_{si}-M'_{\omega i}+L_i\phi'+\sum_{j=1}^{N-1}K_{ij}\theta'_j
\end{aligned}
\right\} \qquad \cdots\cdots (A\cdot2)
$$

where

$$
\left.
\begin{aligned}
&K=\int_A \sigma_z\{(x-x_s)^2+(y-y_s)^2\}dA \\
&L_i=\int_A \sigma_z(h_n r_{ni}+h_s r_{si})\mu_i dA \\
&K_{ij}=\int_A \sigma_z\{(x-x_i)(x-x_j)+(y-y_i)(y-y_j)\}\mu_i\mu_j dA
\end{aligned}
\right\} \qquad \cdots\cdots (A\cdot3)
$$

REFERENCES

1) Bradford, M. A. and Trahair, N. S. : Distortional buckling of I-beams, Proc. ASCE, Vol. 107, No. ST2, pp. 355~377, 1981.
2) Usuki, S. and Hasebe, K. : Local and distortional buckling of thin walled beams based on second order displacement fields, Proc. JSCE, No. 344/I-1, pp. 357~366, 1984 (in Japanese).
3) Fukasawa, Y. and Sugihara, M. : The effects of web distortion on lateral elastic buckling of I-beams, Journal of Structural Engineering, JSCE, Vol. 31 A, pp. 15~23, 1985 (in Japanese).

4) Sugihara, M. and Fukasawa, Y. : Inelastic flexural-torsional buckling strength of I-section members with flexible webs, Reports of the Faculty of Engineering, Yamanashi University, No. 36, pp. 19~25, 1985 (in Japanese).
5) Nishino, F. et al. : Thin-walled members under axial force, bending and torsion, Proc. JSCE, No. 225, pp. 1~12, 1974 (in Japanese).
6) Hikosaka, H. et al. : Finite displacement theory of thin-walled open section member considering cross sectional distortion and its application to problems of elastic stability, Journal of Structural Engineering, JSCE, Vol. 32 A, pp. 265~275, 1986 (in Japanese).
7) Hancock, G. J. : Local, distortional and lateral buckling of I-beams, Proc. ASCE, Vol. 104, No. ST11, pp. 1787~1798, 1978.
8) Desmond, T. P. et al. : Edge stiffeners for thin-walled members, Proc. ASCE, Vol. 107, No. ST2, pp. 329~353, 1981.
9) Takahashi, K. and Mizuno, M. : Distortion of thin-walled open section members (Case of distortion with one degree of freedom and singly symmetrical cross section), Trans. Japan Soc. Mech. Engrs., Vol. 44, No. 378, pp. 460~467, Feb. 1978 (in Japanese).
10) Takahashi, K. and Mizuno, M. : Distortion of thin-walled open section members (Case of distortion with multi degrees of freedom), Trans. Japan Soc. Mech. Engrs., Vol. 45, No. 400, pp. 1545~1553, Dec. 1979 (in Japanese).

(Received May 26 1986)